Shahrood University of Technology

Journal of Hydraulic and Water Engineering (JHWE)

Journal homepage: https://jhwe.shahroodut.ac.ir/

Iranian Hydraulic Association (IHA)

Experimental Results of an Underwater Glider Hydraulic Model Test in Towing Tank of NIMALA

E. Asadi Asrami [1], S. Ardeshiri [2], M. Adjami [3] , M. Moonesun [3,*]

[1] Department of Energy Conversion Takestan, Islamic Azad University, Takestan, Iran
[2] Naval Architecture and Marine Engineering, Malek Ashtar University of Technology, Iran
[3] Department of Civil Engineering, Shahrood University of Technology, Shahrood, Iran

Article Info

Article history:
Received: 16 March 2023
Received in revised form:4 May 2023
Accepted:2 June 2023
Published online:4 June 2023

DOI:
10.22044/JHWE.2023.12852.1006

Keywords
Hydraulic
Model Test
Experiment
Underwater Glider
Towing Tank
Resistance

Abstract

In this article, the hydraulic experimental results of a model of an underwater glider in the marine laboratory (towing tank) of NIMALA are presented. In these hydraulic tests, the resistance force has been extracted at 7 velocities and in three different states (surface and near surface and submerged). Conducting tests in the submerged mode have special hydraulic difficulties because in addition to the model resistance, there are also the struts resistance. It is also important to extend the hydraulic results between the main vehicle and the laboratory model. Today, underwater gliders have many applications in engineering, and accurate calculation of their resistance is very important. These experimental results can be used for validation of CFD modeling in other research works and articles. The main body of the model is taken from Suboff laboratory model, whose validated hydraulic results and hydrodynamic resistance coefficients are available from the laboratory of David Taylor.

1. Introduction

The winged AUVs (Autonomous Underwater Vehicles) are also known as underwater gliders. They don't have a propulsion system at underwater movement but use gravitational and buoyancy forces for advancing forward in a zigzag motion in the vertical plane (Fig.1). A glider in the air can only fall down from a high place once, but in underwater gliders it can be repeated several times by the help of ballast

* *Corresponding author. E-mail address: m.moonesun@gmail.com, Fax: , Tel:+989132111467*

tanks and the hydroplanes. Depending on the type of mission defined for them, the duration of the mission and the range of these trends will be determined (Komerska et al., 1999; Azcueta, 2003; Blidberg et al., 2004; Hoque et al., 2017; Yan et al., 2023). If there are defined times of about a few hours for their mission, they will have no particular problem with power supply but for a mission of about a week to several months, powering these AUVs will be a serious challenge and their mission will be severely restricted (Duarte et al., 2003). The solar energy is a sustainable and reliable source. In order to powering these types of AUVs, using solar energy can be a good solution for increasing the range and duration of the process for several weeks to even months (Asadi Asrami and Moonesun; Blidberg et al., 1997; Ageev et al., 2002; Griffiths, 2002; Crimmins et al., 2006; De Luca et al., 2016; Mateja et al., 2023). The technical notes of an Iranian sample (Arya) designed by the authors of this article are also mentioned here.

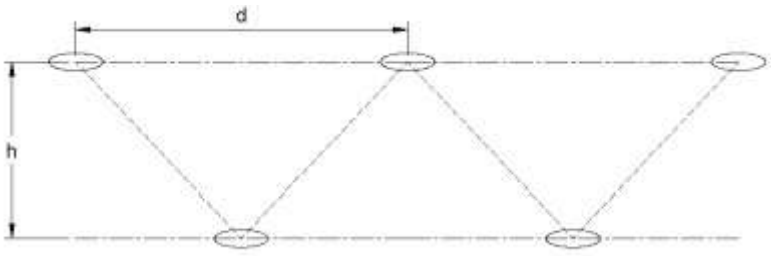

Figure 1. Zigzag motions in the vertical plane for forward advancing

2. Material and methods

2.1. Specifications of Arya Solar AUV Model

Arya has the length of about 1.2 meters with the main body of SUBOFF type, which its hydraulic experimental data is available (Asadi Asrami et al., 2021). The model of Arya is made in real dimensions and scale factor of 1:1 by the material of special wood with the length of 1.2 meters (Fig. 2). Solar submarines usually have small dimensions, so there is no need to scale and make the model smaller. Consequently, there is no worries about the similarity of the boundary layer between the main AUV and the hydraulic experimental model; therefore, here, any flow disturbing method is not used. In this case, there are no more errors of extending the model results to the original. The material and density of the model is so considered that waterline could be easily adjusted at surface draft. The surface of the body is primed and painted (Fig. 3) to gain a minimum roughness according to ITTC standard procedure 7.5-02-03-01.4 (revision 04-2017).

The body has two hydroplanes on the both sides of the body with the cutted NACA0015 cross-section. The exact dimensions of the model are shown in Figure 2.

Table 1. Main dimensions of solar AUV and struts (mm)

AUV components	Dimensions (mm)
Overall length	1200
Width	860
Body middle section maximum diameter	140
Wing root chord length	614
Wingtip chord length	487
Wing camber thickness	52.66
Rudder root chord length	55.32
Rudder tip chord length	42
Rudder camber thickness	6.3
Maximum strut diameter	65
Minimum strut diameter	20
Strut overall height	1000

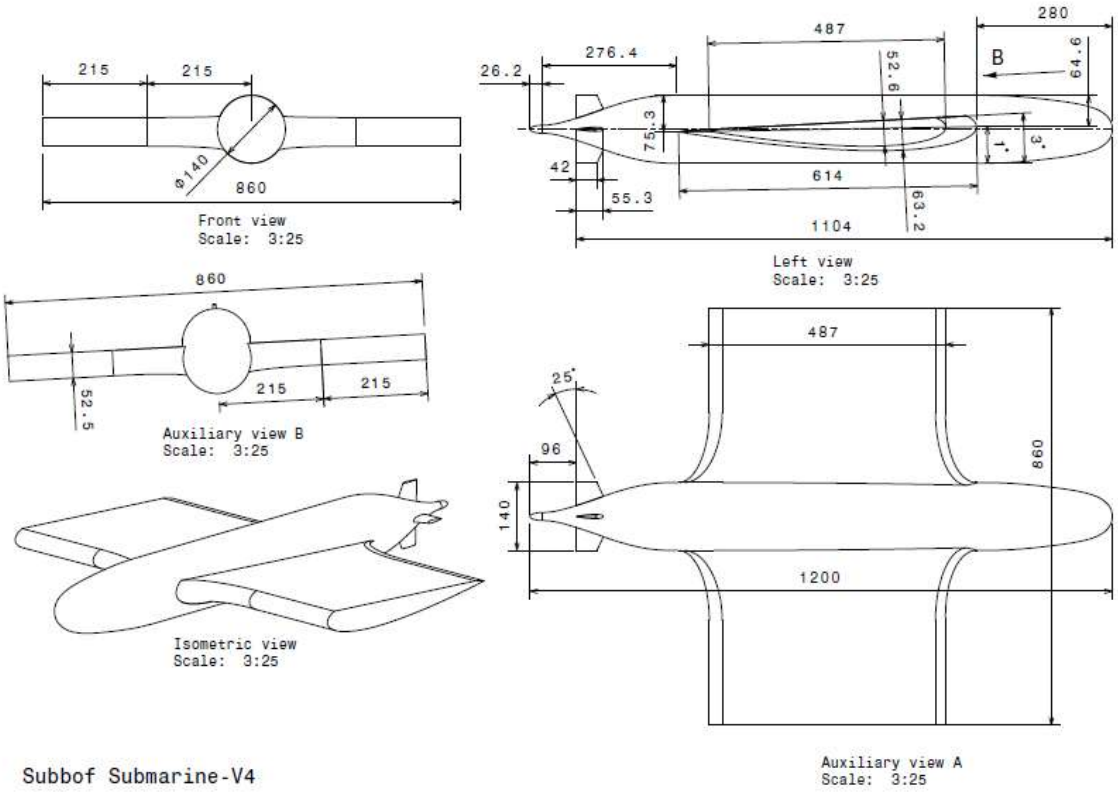

Figure 2. Detailed dimensions of the model

Figure 3. Construction of the model

2.2. Experiment Procedure of Model Resistance

A solar AUV, firstly in surface mode, absorbs solar radiation through its photovoltaic panels; when its batteries are charged, it sinks in the water for various missions. To estimate AUV required energy, we have to evaluate hydrodynamic forces acting on the AUV's body for a test model. The flow around an AUV that uses a solar energy source is explored in this study. A 1:1 scale model of this form of vehicle was created and built out of Abies wood, and after final surface polishing and painting, it was tested at the National Iranian Marine Laboratory (NIMALA). The two wings were each based on the NACA0015 cross-sectional profile to create a proper lift and place the panels. The four astern hydroplanes at a 90-degree angle to each other were likewise built from the same section. The center body was a SUBOFF model as well. The simulation results for three depth-to-diameter ratios with varying diameters ($\frac{h}{d} = 3.6 , 4.5 , 5.2$), and in the Reynolds number range (calculated in terms of body length) $Re = 2.4 \times 10^5 \sim 1.4 \times 10^6$. The forces acting on the two struts, as well as the forces acting on the body without the struts, were calculated individually and independently by numerical simulation to get the net forces operating on the model body. The resistance force was lower in both the body without struts and the individual struts cases than in the body with struts. This difference is due to the induced resistance force. The lift forces caused by the presence of extended wings (which are where photovoltaic panels are installed) and astern hydroplanes were also examined using the CFD method, and the shapes of the wave profiles derived from the CFD method and test at any velocity and depth were also

compared. To achieve the characteristics of the resistance and the waveform formed during the test of the studied model, a model made of Abies was constructed by CNC lathes with a 1:1 scale vessel, following the ITTC 7.5-02-03-01.4 (revision 04-2017) recommendations, and then the surface was polished and painted. For a higher accuracy, the model's four astern hydroplanes were made utilizing the RP (rapid prototype) technique. The astern hydroplanes and the large wings, which act as mounting components for the photovoltaic panels, were built separately and then assembled into the body. The body linked to the struts can be seen in Figure 4. Because the body is made of wood, lead is used to fully immerse it (Zheng et al., 2017; Divsalar, 2020). This lead addition is necessary to maintain balanced weight distribution in the vessel geometry. Struts are regulated in height to provide the possibility of their wetted height measurement. The model's movement within the towing tank is restricted to a single degree of freedom and a straight line. Struts connect the model to two two-component dynamometers (Fig. 4). This laboratory's towing tank is 402 meters long, 6 meters wide, and 4.5 meters deep. Its trolley velocity ranges from 0.1 to 19 m/s in two modes of motion: slow motion (0.5 to 5 m/s) and fast motion (4.5 to 19 m/s). The passenger trolley has a capacity of 5 people and dimensions of 7.6 7.6 meters. The model is towed at a constant pace at all six velocities and three depths during the test. The forces acting on the body and struts at each velocity are measured with a force transducer and recorded on a computer.

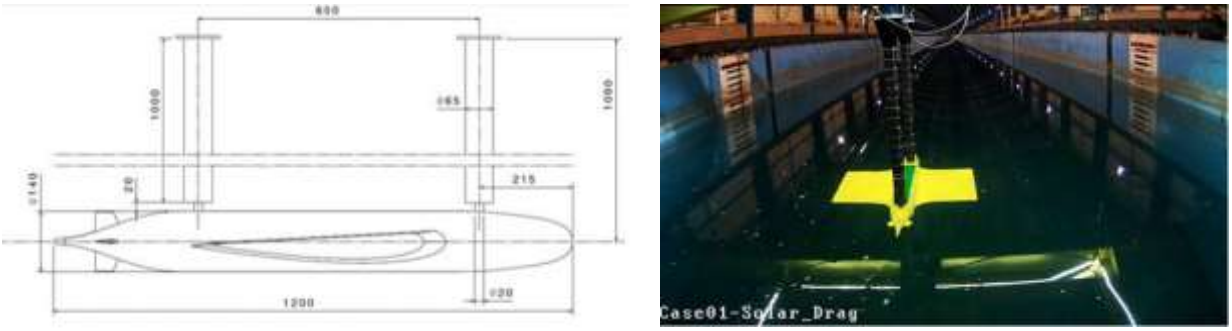

Figure 4. A view of the NIMALA towing tank and model test attachment to the struts

Table 2. Values of the test velocities and the corresponding Reynolds and Froud numbers

Velocity (m/s)	Re	Fr
0.2	238851	0.05829
0.4	477702	0.11658
0.6	716554	0.17487
0.8	955405	0.23316
1	1194257	0.29145
1.2	1433108	0.34974
1.4	1671959	0.40803

4. Results and Discussions

4.1. Model Test at surfaced condition

The configuration of experiments in 7 different velocities at surfaced condition are shown in Figures 5 and 6. The resistance results are shown in Table 3. The resistance value increases drastically at the velocities more than 1 m/s. The analysis of the reason can be stated as below. In velocities more than 1 m/s, the body is completely submerged by large angle of pitch due to the foil section of the hydroplanes. This phenomenon is clearly illustrated at velocity of 1.4 m/s. Complete submersion of the body increases the wetted area surface and frictional resistance. Increasing the pitch angle causes flow separation on the body and increasing the viscous pressure resistance. Due to this phenomenon, the maximum velocity of Arya at surface condition is defined equal to 1 m/s. The wetted area at surface condition is 0.58 m^2.

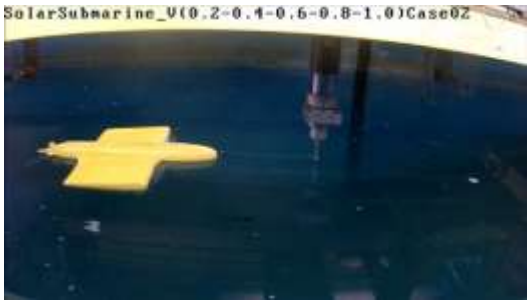

V=0.2 m/s

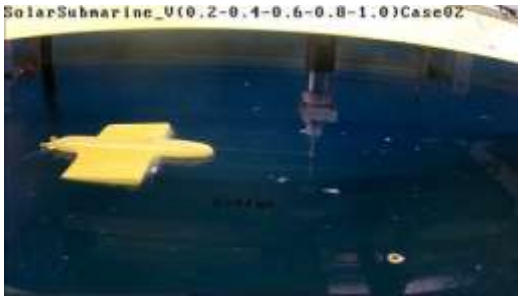

V=0.4 m/s

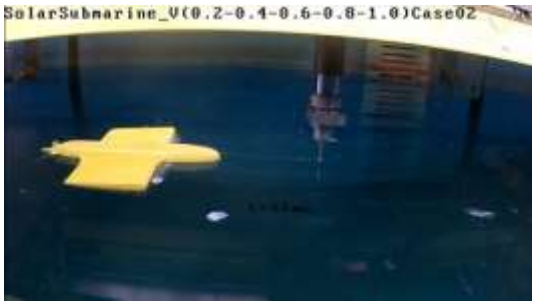

V=0.6 m/s

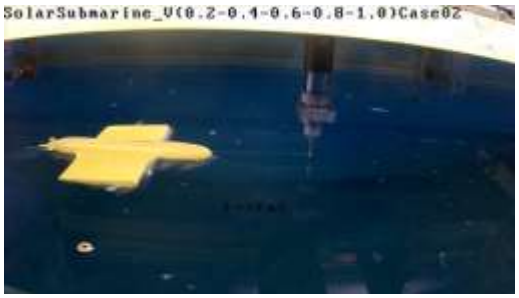

V=0.8 m/s

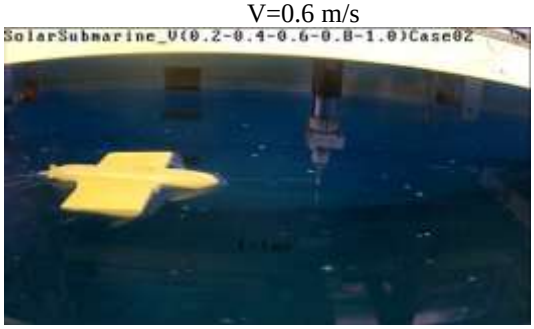

V=1 m/s

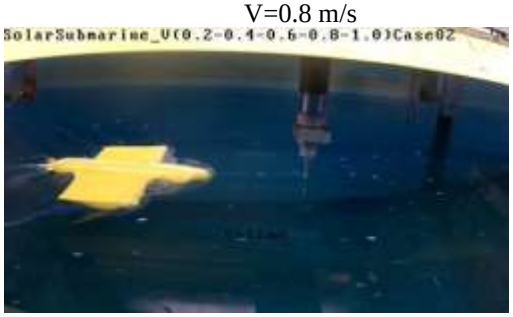

V=1.2 m/s

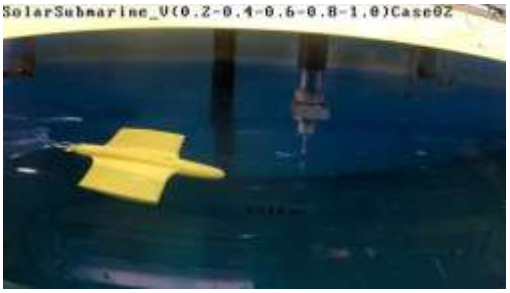

V=1.4 m/s

Figure 5. Wave pattern around the body at surfaced condition:

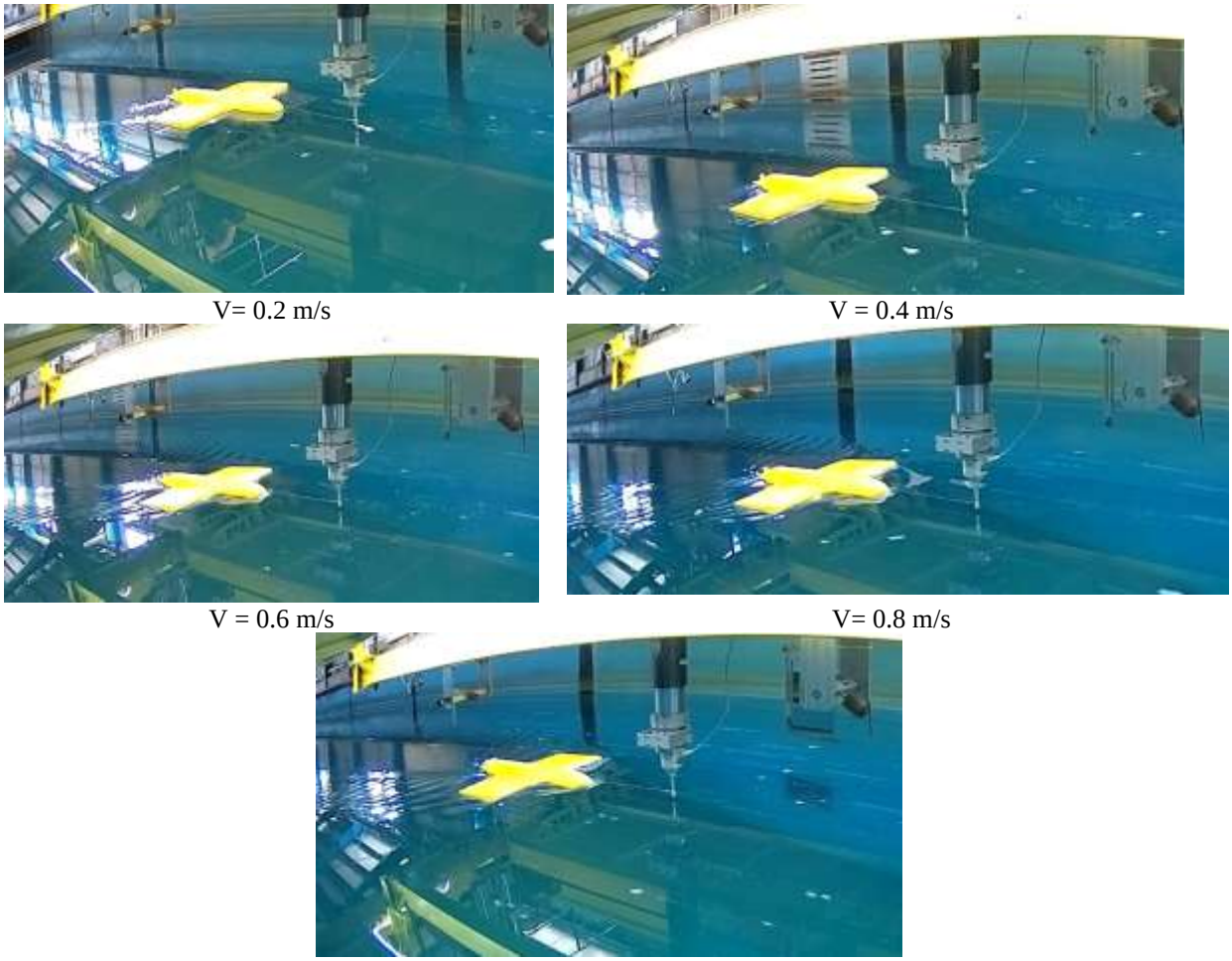

Figure 6. Model test at surfaced condition in 7 velocities

Table 3. Resistance and Resistance coefficient results in seven velocities

V(m/s)	R (N)	C(-)
0.2	0.098	0.0084
0.4	0.38	0.0082
0.6	0.86	0.0083
0.8	2.20	0.0119
1	5.25	0.019
1.2	40.54	0.0485
1.4	41.05	0.0361

4.2. Model test at submerged

The configuration of experiments in 7 different velocities at three different depths are shown in Figure 7. The resistance results are shown in Table 4 and 5 for body and two struts. To obtain the net resistance of the model, the resistance of the struts and interaction effects should be subtracted from the above results. For estimating the interaction effect (between the body and

struts), some CFD modeling is required. The CFD modeling is not the subject of this article but these results can be used for further research and validation of CFD modeling in the design of underwater gliders. The wetted area at submerged condition is 1.16 m^2.

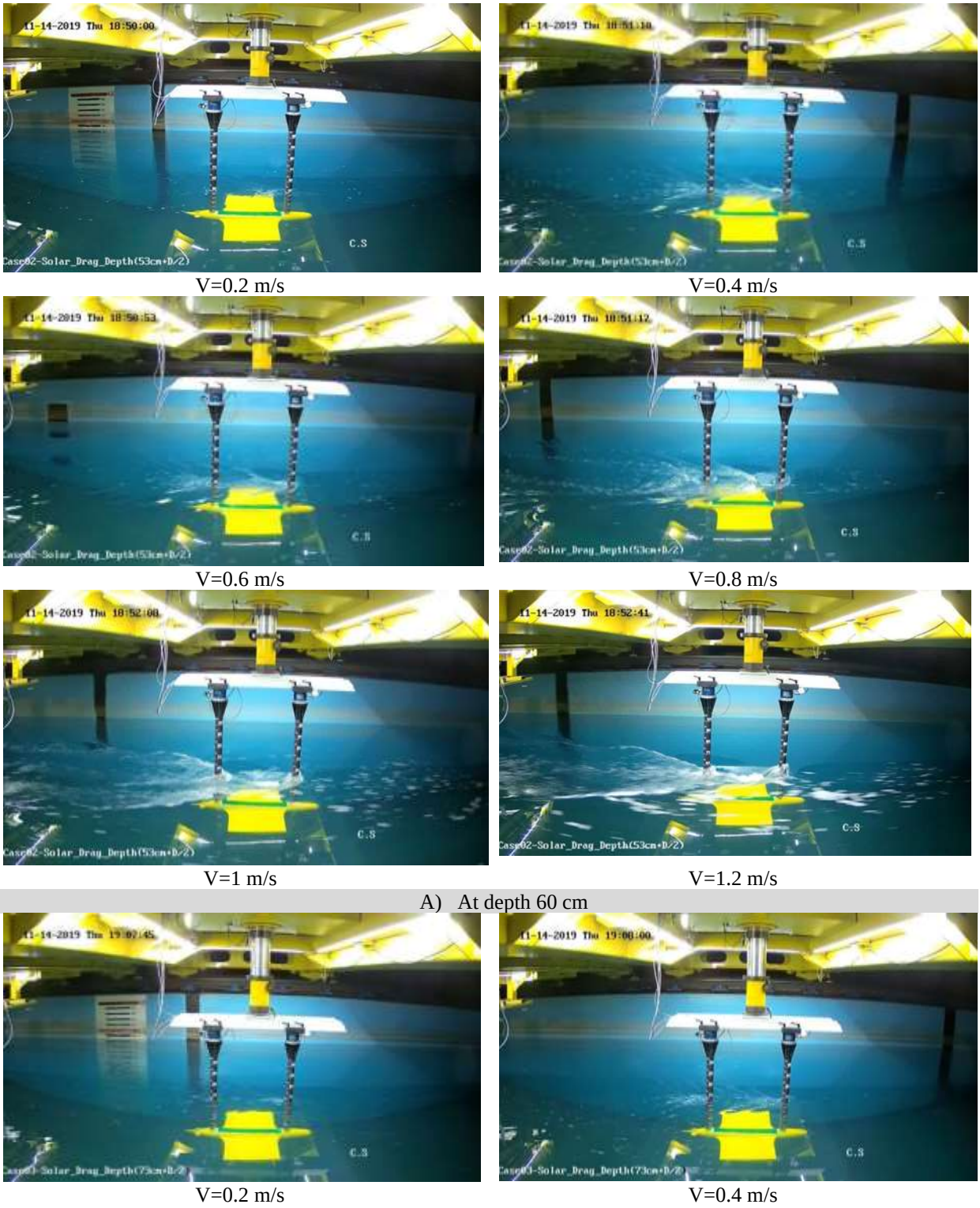

V=0.2 m/s V=0.4 m/s

V=0.6 m/s V=0.8 m/s

V=1 m/s V=1.2 m/s

A) At depth 60 cm

V=0.2 m/s V=0.4 m/s

Figure 7. Model test at submerged condition

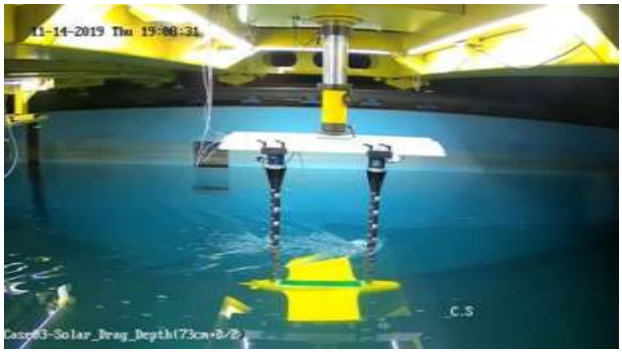
V=0.6 m/s

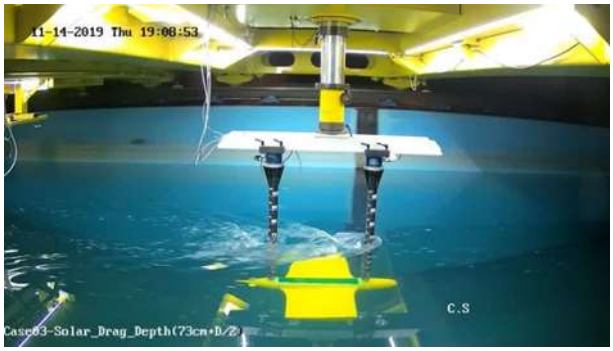
V=0.8 m/s

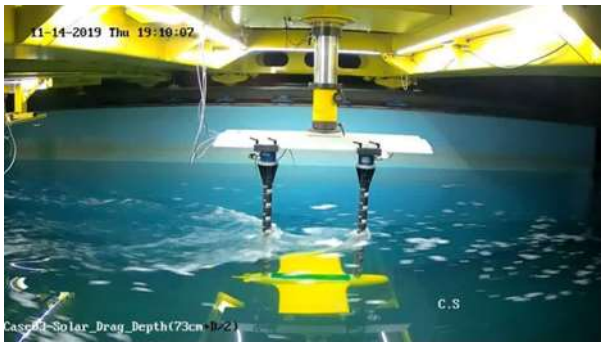
V=1 m/s

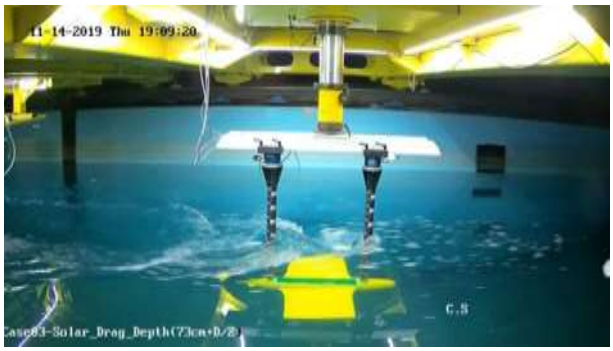
V=1.2 m/s

B) At depth 70 cm

Figure 7. (Continued)

Table 4. Resistance (Body+Struts) [N]

V(m/s)	H=41cm + 0.5d=48 cm	H=53cm + 0.5D=60 cm	H=63cm + 0.5d= 70 cm
0.2	0.20	0.24	0.291
0.4	0.71	0.97	1.1
0.6	1.5	2.15	2.1
0.8	2.9	3.2	3.6
1	4.7	5.05	5.7
1.2	6.1	6.9	7.67

Table 5. Resistance coefficient (Body+Struts)

V(m/s)	H=41cm + 0.5d=48 cm	H=53cm + 0.5D=60 cm	H=63cm + 0.5d= 70 cm
0.2	0.043	0.052	0.063
0.4	0.039	0.051	0.057
0.6	0.037	0.05	0.05
0.8	0.037	0.044	0.049
1	0.037	0.044	0.052
1.2	0.036	0.042	0.048

5. Conclusions

In this article, the results of the model test on an underwater glider at surface, underwater and near the water surface were presented. These results were presented for seven different velocities that can be used for further

research and validation of CFD modeling in the design of underwater gliders. These activities are performed in NIMALA laboratory.

Data Availability

The data used to support the findings of this study is available from the corresponding author upon request.

Conflicts of Interest

The authors declare that they have no conflicts of interest regarding the publication of this paper.

Acknowledgement

We gratefully acknowledge the support and funding provided by the Shahrood University of Technology to conduct this research work.

References

Ageev, M.D., Blidberg, D.R., Jalbert, J., Melchin, C.J., and Troop, D.P., 2002. Results of the evaluation and testing of the solar powered AUV and its subsystems, Proceedings of the 2002 Workshop on Autonomous Underwater Vehicles, 2002. IEEE, pp. 137-145.

Asadi Asrami, E., and Moonesun, M., Numerical and experimental investigation of the hydrodynamic Lift and Drag coefficients of a solar-powered AUV in near-surface mode. *International Journal of Maritime Technology*, pp. 1-26.

Asadi Asrami, E.A., Moonesun, M., and Abi, F.A., 2021. Computational fluid dynamics and experimental hydrodynamic analysis of a solar AUV. *Computer Assisted Methods in Engineering and Science*, 28(1), pp. 57-77.

Azcueta, R., 2003. Steady and unsteady RANSE simulations for planing crafts. *FAST Sea Transportation, Ischia, Italy*.

Blidberg, D.R., Chappell, S., and Jalbert, J.C., 2004. Long endurance sampling of the ocean with solar powered AUV's. *IFAC Proceedings Volumes*, 37(8), pp. 561-566.

Blidberg, D.R., Jalbert, J., and Ageev, M.D., 1997. Some design considerations for a solar powered AUV; Energy management and its impact on operational characteristics, International Symposium On Unmanned Untethered Submersible Technology. Citeseer, pp. 50-59.

Crimmins, D.M., Patty, C.T., Beliard, M.A., Baker, J., Jalbert, J.C., Komerska, R.J., Chappell, S.G., and Blidberg, D.R., 2006. Long-endurance test results of the solar-powered AUV system, OCEANS 2006. IEEE, pp. 1-5.

De Luca, F., Mancini, S., Miranda, S., and Pensa, C., 2016. An extended verification and validation study of CFD simulations for planing hulls. *Journal of Ship Research*, 60(02), pp. 101-118.

Divsalar, K., 2020. Improving the hydrodynamic performance of the SUBOFF bare hull model: a CFD approach. *Acta Mechanica Sinica*, 36(1), pp. 44-56.

Duarte, C., Martel, G., Eberbach, E., and Buzzell, C., 2003. A common control language for dynamic tasking of multiple autonomous vehicles, Proc. of the 13th Intern. Symp. on Unmanned Untethered Submersible Technology UUST, pp. 24-27.

Griffiths, G., 2002. Technology and applications of autonomous underwater vehicles, 2. CRC Press.

Hoque, M.A., Karim, M.M., and Rahman, A., 2017. Simulation of water wave generated by shallowly submerged asymmetric hydrofoil. *Procedia engineering*, 194, pp. 38-43.

Komerska, R., Chappell, S., Peng, L., and Blidberg, D., 1999. Generic behaviors as an interface for a standard AUV command & monitoring language. *AUSI Technical Report 9904–01*.

Mateja, K., Skarka, W., Peciak, M., Niestrój, R., and Gude, M., 2023. Energy Autonomy Simulation Model of Solar Powered UAV. *Energies*, 16(1), pp. 479.

Yan, Z., Yan, J., Wu, Y., Cai, S., and Wang, H., 2023. A novel reinforcement learning based tuna swarm optimization algorithm for autonomous underwater vehicle path planning. *Mathematics and Computers in Simulation*, 209, pp. 55-86.

Zheng, H., Wang, X., and Xu, Z., 2017. Study on hydrodynamic performance and CFD simulation of AUV, 2017 IEEE International Conference on Information and Automation (ICIA). IEEE, pp. 24-29.